A Crossed Molecular Beam Study of the Reaction $O(^1D) + HI \rightarrow IO + H$

Michele Alagia, Nadia Balucani, Piergiorgio Casavecchia,* and Gian Gualberto Volpi

Dipartimento di Chimica, Università di Perugia, 06123 Perugia, Italy

Received: February 25, 1997; In Final Form: May 19, 1997⊗

The angular and velocity distributions of the IO product from the reaction $O(^1D) + HI$ have been obtained in crossed beam experiments at collision energies, E_c, of 4.7 and 13.6 kcal/mol. The product center-of-mass angular distribution is found to be nearly backward−forward symmetric, with forward scattering favored. The forward to backward scattering ratio increases with increasing E_c, from which it is deduced that the reaction occurs via an intermediate complex having a lifetime comparable to its rotational period. Within the "osculating" model for chemical reactions, the complex lifetime is estimated to be 4 and 1 ps at low and high E_c, respectively. A large fraction (0.55 at low E_c and 0.46 at high E_c) of the total available energy was found to be released into product translational energy. Comparison with the dynamics of the analogous reactions $O(^1D) + HCl$ and $O(^1D) + HBr$ is carried out: similarities as well as differences are noted and discussed in terms of the potential energy surfaces for reaction. From comparison of signal intensities and the previously estimated lower limits to the branching ratio of the relative cross sections for XO + H and OH + X channels in the $O(^1D) + HX$ (X = Cl, Br) reactions, it is concluded that the H-displacement pathway accounts for a significant fraction of the overall reaction also in the case of $O(^1D) + HI$.

Introduction

The reactions of atomic oxygen, in both the ground state $O(^3P)$ and the first electronically excited state $O(^1D)$, with halogenated compounds are of interest in determining the impact of anthropogenic surface release of halogen-containing molecules on the atmosphere and especially on the ozone natural balance. They are also of relevance in the combustion chemistry of halogenated compounds, as for instance in their use as fire extinguishers. Among these reactions, those with hydrogen halides are particularly simple and can be considered as prototypes; indeed, they comprise a class of three-atom reactions that are amenable to detailed experimental and theoretical investigation. While the reactions of HCl and HBr with both $O(^3P)$ and $O(^1D)$ have been recently studied from both kinetics[1−4] and dynamics[5−9] standpoints, little information is available on the reaction of HI with $O(^3P)$[3,10,11] and none on the reaction with $O(^1D)$.

In previous work from this laboratory we reported the results of direct dynamical investigations, using the crossed molecular beam (CMB) scattering method, on the reactions $O(^1D) + HCl$,[5] HBr,[7] and CF_3Br,[12] relative to the XO (X = Cl, Br) formation channel. Here we extend these studies to the next member of the $O(^1D) + HX$ series, namely, the reaction $O(^1D) + HI$. This reaction can proceed via two competing pathways:

$$O(^1D) + HI \rightarrow IO + H \qquad \Delta H^\circ_0 \approx -30 \text{ kcal/mol} \qquad (1a)$$

$$\rightarrow OH + I \qquad \Delta H^\circ_0 = -75.8 \text{ kcal/mol} \qquad (1b)$$

Heats of reaction were derived from the data of ref 13, with the exception of $\Delta H^\circ_{f,0}$ (IO) (see below). All products of reaction 1 may be catalytically active species in ozone chemistry. Recently, a growing concern for the potential role of iodine in atmospheric chemistry has motivated experimental and theoretical studies of the likely relevant iodine "active" and "reservoir" forms and iodine involving reactions. In 1980, Chameides and Davis[14] first pointed out that, while the active forms of chlorine and bromine contribute to *stratospheric ozone* depletion, the *tropospheric ozone* balance may be affected significantly by iodine compounds. In fact, in the tropospherical environment the thermal and photochemical stability of the principal inorganic reservoirs of chlorine and bromine (i.e., HCl, HBr, HOCl, HOBr, $ClONO_2$, and $BrONO_2$) greatly limits the impact of these halogens on the ozone budget. On the contrary, iodine reservoir species are easily photodissociated in the near-UV and visible region (since the bonds involving iodine are generally weak), leading to the rapid release of active iodine; the dominant reaction of the formed iodine atoms seems to be that with O_3

$$I + O_3 \rightarrow IO + O_2 \qquad (2)$$

while the IO radical returns back to I primarily by photodissociation

$$IO + h\nu\ (\lambda = 4550 \text{ Å}) \rightarrow I + O \qquad (3)$$

or by reaction

$$IO + NO \rightarrow I + NO_2 \qquad (4)$$

The IO radical can also react to form reservoir species through

$$IO + NO_2 \rightarrow IONO_2 \qquad (5)$$

$$IO + HO_2 \rightarrow HOI + O_2 \qquad (6a)$$

$$\rightarrow HI + O_3 \qquad (6b)$$

Of all the inorganic reservoirs, HI is the least photolabile (its photochemical lifetime is ≈1−2 h during the day), and its reaction with OH radicals

$$HI + OH \rightarrow H_2O + I \qquad (7)$$

is the main gas-phase HI loss process. Reaction 7 regenerates the active form of I. Many other reactions, including photodissociation of HOI, were postulated to occur, giving rise to a net loss of tropospheric ozone. Since most of these reactions were not studied at that time, the potential role of iodine was

---

⊗ Abstract published in *Advance ACS Abstracts,* July 15, 1997.

S1089-5639(97)00697-X CCC: $14.00

just proposed by the authors,[14] who made a call for experimental studies and field measurements in order to assess the model. Subsequently, most of the reactions involved and the photochemical processes proposed were studied and rate coefficients determined.[15] Lately, there has been a renewed interest in iodine chemistry stemming from the recent assessment that iodine could account for the observed depletion of lower stratospheric ozone (below 20 km, altitudes where chlorine and bromine are not very effective for ozone destruction in contrast to iodine) at midlatitudes.[16] Studies of convective transport have shown that vertical transport of iodine-containing molecules can be significant, allowing the photochemically short-lived iodine compounds to reach the upper troposphere and even the lower stratosphere. Due to the instability of its reservoir species, the efficiency of iodine released in the stratosphere for ozone depletion near 15−20 km would be more than 1000 times greater than that of Cl, leading to the conclusion that even a very small amount of iodine could cause significant O_3 destruction.[16] Actually, the iodine role in ozone depletion is thought to be of enhancing the effect of the human-released chlorine and bromine, through the interhalogen reactions IO + ClO and IO + BrO.[16] The main source of atmospheric iodine is natural: methyl iodide, chloroiodomethane, and diiodomethane are thought to be produced by marine biota, such as phytoplankton, kelp, and macroalgae; in particular, iodocarbons generated by biomass burning could contribute significantly to the iodine reaching directly the stratosphere.[16]

The fraction of stratospheric iodine that is expected to reside in the form of HI is ≈0.5%.[16] Even though reaction (1) is not thought to play a major role either in the tropospheric ozone budget (where reaction 7 is dominant) or in the stratospheric one, in both environments $O(^1D)$ is significantly present since it is the product of ozone photodissociation. All the products of reaction 1 are active forms in ozone depletion, so that reaction 1 could represent an alternative way for iodine to pass from the reservoir HI to active radicals. Moreover, reaction 1 can be considered as prototypical of the reactions of $O(^1D)$ with simple iodine-containing molecules, a class of compounds which is now being considered as a substitute for halon fire suppressants.[16b] The rate constant of reaction 1 has never been determined; recent kinetic studies provided room-temperature rate constants for the analogous reactions $O(^1D) + HCl$ and $O(^1D) + HBr$ (and also $O(^1D) + HF$).[4a] Comparison with the rate constants for the reactions $O(^3P) + HCl$ and $O(^3P) + HBr$ shows that the electronic excitation of the oxygen atom leads to an increase of 6 and 4 orders of magnitude for HCl and HBr, respectively. For $O(^3P) + HI \rightarrow OH + I$ it was found[3] $k_{298} = 1.62 \times 10^{-12}$ cm^3 molecule^{-1} s^{-1}, quite larger than 3.8×10^{-14} and 1.3×10^{-16} cm^3 molecule^{-1} s^{-1}, which are the k_{298} values for $O(^3P) + HBr$ and $O(^3P) + HCl$, respectively.[1−3] Therefore, the rate constant for reaction 1 is expected to be at least comparable to those of the reactions $O(^1D) + HCl$ and $O(^1D) + HBr$, especially if one considers that the reactions of $O(^1D)$ with most compounds usually occur with near gas kinetic frequency due to the fact that they take place on a singlet ground state potential energy surface (PES) with virtually zero activation energy. It should be noted that for the $O(^3P) + HX$ (X = Cl, Br) reactions the OH + X channel is exoergic and the H + XO channel strongly endoergic. Instead, both channels are exoergic for $O(^1D)$; in particular, kinetic[4] and dynamic[5,6d,7,9a] studies indicate that the H-displacement channel in the $O(^1D) + HX$ (X = Cl, Br) reactions accounts for a considerable fraction of the overall reaction.

Dynamical studies of $O(^1D)$ reactions with simple molecules also address the important issue of the role of electronic excitation on the reaction dynamics of nonmetal atoms. The reactions of $O(^1D)$ with H−X molecules (where X = H, Cl, Br, I, OH, SH, CH_3) are postulated to proceed through the formation of a strongly bound complex, HOX, following the insertion of $O(^1D)$ into a bond of the colliding molecule.[17] However, the lifetimes of the complexes and the dynamics of their dissociation are not well-known yet. In particular, the nonstatistical energy partitioning observed in most of the $O(^1D)$ reactions pointed to a precluded equilibration of the available energy among the degrees of freedom of the complexes;[6f] in other words, the randomization of energy of the complex does not occur within the time scale required for its decomposition. For instance, in the case of the reaction $O(^1D) + CH_4$, even though the decay time of the CH_3OH formed from the photolysis of the $CH_4{\cdot}O_3$ van der Waals adduct was found[18] to be 3 ps at $E_c \approx 13$ kcal/mol (a value comparable to the lifetime calculated from Rice−Ramsperger−Kassel−Marcus theory for the dissociation of methanol at the level of excitation of the experiment), the OH product internal energy distribution is not found to be statistical.[19] The results presented below, together with the information obtained in this laboratory on the related reactions $O(^1D) + H_2$,[20] $O(^1D) + HCl$,[5] $O(^1D) + HBr$,[7] $O(^3P,^1D) + H_2S$,[21] and $O(^3P,^1D) + CH_3I$,[22] provide a useful database also for comparison with theory. It should be noted that reactions involving $O(^3P,^1D)$ with simple molecules are good candidates for studies investigating the role of multiple potential energy surfaces and nonadiabatic effects on chemical reaction dynamics.

The study reported here has been carried out using the powerful CMB method pioneered by Professor Y. T. Lee, together with Professor D. R. Herschbach.[23] Also, the method used for generating intense continuous supersonic beams of $O(^1D)$ atoms, which is crucial for the present studies, has been originally developed in Lee's laboratory.[24] It is our pleasure and most appropriate to dedicate this paper to Professor Lee on the occasion of his 60th birthday.

Experimental Section

The scattering experiments were carried out on the universal crossed molecular beam apparatus of Perugia, which is an implementation for reactive scattering studies of the high-resolution machine previously used for measuring elastic and total (elastic + inelastic) differential cross sections for atom−atom and atom−molecule collisions.[25] The apparatus has been described in detail elsewhere,[25,26] and only a brief description necessary to understand the present experiments is given here. Two well-collimated supersonic beams of the reactants, after two stages of differential pumping, are crossed at 90° under single-collision conditions in a large scattering chamber maintained below 5×10^{-7} mbar. The reaction products are detected by an electron bombardment ionization quadrupole mass spectrometer which can rotate in the plane of the two beams around their intersection axis (i.e., around the collision region). The ionizer is mounted on a liquid nitrogen cooled OFHC copper chamber, which is kept in the 10^{-11} mbar region by extensive ion-, turbo-, and cryo-pumping and represents the innermost region of a triply differentially pumped ultrahigh-vacuum rotatable chamber.

The seeded supersonic atomic oxygen beams, containing $O(^1D)$ and ground-state $O(^3P)$, were generated by a high-pressure, radio-frequency (rf) discharge nozzle source similar in design to that described by Sibener et al.[24] and which has been optimized for $O(^1D)$ production.[5,7,20,21,26] Two $O(^1D)$ beams with different translational energies were produced in order to vary the relative collision energy of the experiment.

By discharging 350 mbar of a 5% O_2 in helium gas mixture through a 0.26 mm diameter quartz nozzle at 250 W of rf power, a beam with peak velocity of 2854 m/s and speed ratio of 7.0 was obtained. By discharging 350 mbar of a 5% O_2 in neon gas mixture through the same quartz nozzle at 290 W of rf power, a beam with peak velocity of 1661 m/s and speed ratio of 6.2 was produced. The angular divergence is 2.3° in both cases. Using the fast and slow beams of $O(^1D)$, relative collision energies, E_c, of 13.6 and 4.7 kcal/mol, respectively, were obtained (see below). Due to the very efficient coupling of the rf power to the plasma, high degrees of molecular dissociation are achieved (>80% and >90% with the helium and neon mixture, respectively). The oxygen beams contain a very large fraction of ground-state $O(^3P)$, but this species does not interfere since the collision energies of the present experiments are not sufficient to overcome the large endoergicity of the reaction $O(^3P) + HI \rightarrow IO + H$ ($\Delta H°_r \approx 15.4$ kcal/mol).

Supersonic beams of HI were generated by expanding pure HI through a 100 μm diameter stainless steel nozzle. For the experiment at $E_c = 13.6$ kcal/mol the HI stagnation pressure was 0.35 bar, and the resulting peak velocity and speed ratio were 370 m/s and 8.1, respectively; for the experiment at $E_c = 4.7$ kcal/mol slightly different experimental conditions, such as the HI stagnation pressure which was 0.32 bar, gave a peak velocity of 369 m/s and a speed ratio of 8.0. The angular divergence was 2.9° in both cases. Under these expansion conditions HI clustering was negligible. Because of the significant rotational cooling during supersonic expansion (a rotational temperature of about 16 K is estimated, assuming equilibrium between translational and rotational degrees of freedom), the HI molecules in the beam are expected to be in the lowest few rotational states of the ground vibrational level, and therefore the internal energy of the molecular reactant contributes negligibly (<0.1 kcal/mol) to the total available energy.

Angular distributions of the IO product were obtained by taking at least five scans of 50 s counts at each angle. The HI beam was modulated at 160 Hz by a tuning-fork chopper for background subtraction. Velocity analysis of the beams was carried out by conventional "single-shot" time-of-flight (TOF) techniques, using a high-speed multichannel scaler and a CAMAC data acquisition system controlled by a personal computer. Velocity distributions of products were obtained at 11 different angles at $E_c = 13.6$ kcal/mol and at 12 different angles at $E_c = 4.7$ kcal/mol using the cross-correlation TOF technique[27] with four 127-bit pseudorandom sequences. High time resolution was achieved by spinning the TOF disk, located at the entrance of the detector, at 393.7 Hz corresponding to a dwell time of 5 μs/channel. The flight length was 23.6 cm. Counting times varied from 15 to 60 min depending upon the signal intensity.

Results and Analysis

Under the experimental conditions of the present study, we were able to observe only the IO product from reaction 1a, while the signal from the kinematically unfavored OH, produced in the reaction channel 1b, could not be detected. In fact, as stated by linear momentum conservation, the light OH from the strongly exothermic channel 1b moves very fast and is spatially distributed in a very broad laboratory angular range, since its scattering partner is the heavy I atom; on the contrary, the heavy IO from the significantly less exothermic channel 1a has a much lower center-of-mass (c.m.) velocity and is confined in a narrow lab angular range around the c.m., since its scattering partner is the light H atom. This leads to a strong enhancement of the IO number density in the lab frame with respect to that of OH. From the failure to detect the OH, only an indication about the ratio of cross sections of channel 1a and 1b could be given (see below).

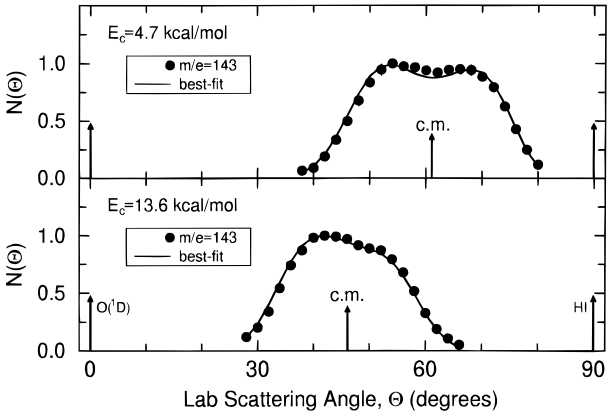

Figure 1. Laboratory angular distributions of the IO product from the $O(^1D) + HI$ reaction at two different collision energies, E_c. Solid lines: calculation with best-fit c.m. translational energy and angular distributions of Figure 3.

The angular distributions of the IO product, detected at $m/e = 143$, for the collision energies of 13.6 and 4.7 kcal/mol are shown in Figure 1. The error bars are also reported when they exceed the size of the dots. The IO^+ signal at the peak of the angular distribution was 2700 counts/s with a signal-to-noise ratio (S/N) of 195 (the ionizer emission current was 5 mA) at $E_c = 13.6$ kcal/mol using 50 s counting times; at the low E_c the peak signal was lower (650 counts/s with S/N = 55) mainly due to the lower intensity of $O(^1D)$ in the Ne seeded beam. The solid lines in Figure 1 show the calculated best fit (see below). The product time-of-flight distributions at the two energies are reported in Figure 2a,b together with the results of the best-fit calculations (see below); they have been normalized to the relative intensities at each angle. The angular distribution at $E_c = 13.6$ kcal/mol shows some kind of structure around the c.m. position angle ($\Theta_{c.m.} = 46°$), with a pronounced shoulder at angles smaller than $\Theta_{c.m.}$. The angular distribution at the lower E_c appears, instead, almost symmetric with respect to $\Theta_{c.m.}$ (in this case $\Theta_{c.m.} = 61°$ because of the lower $O(^1D)$ beam peak velocity), but again a small preference for scattering at angles smaller than $\Theta_{c.m.}$ can be observed. The TOF spectra at both E_c display also bimodality at angles close to $\Theta_{c.m.}$. This fact and the large width of the lab angular distributions (especially considering that IO is a very heavy particle) suggest that the product translational energy distribution peaks away from zero and that the fraction of available energy released in translation is large.

Data at both energies were analyzed by using a forward convolution trial-and-error fitting procedure where the c.m. angular and energy distributions are input as trial functions.[28,29] The corresponding laboratory angular and TOF distributions are then calculated and compared to the experimental data. The experimental resolution broadening, due to the TOF disk and detector slit sizes, disk velocity and ionizer length, and spread in beam velocities and angular divergences, is taken into account. The original trial function is adjusted and the process repeated until a satisfactory fit is obtained to both the TOF spectra and the angular distributions. The energy dependence of the reaction cross section has been taken into account in the data analysis. For a reaction like this, which is thought—by analogy with the reactions $O(^1D) + HCl$ and $O(^1D) + HBr$—to occur without threshold and dominated by long-range forces in the entrance channel, the centrifugal barrier model[30] predicts a

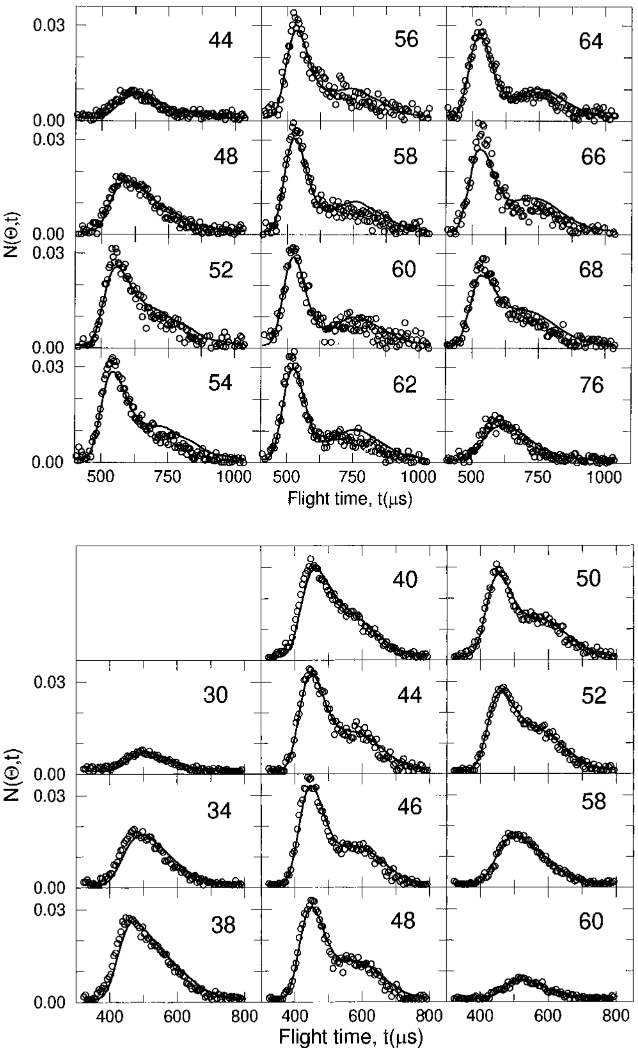

Figure 2. Time-of-flight spectra of the IO product at the indicated laboratory angles for (a, top) $E_c = 4.7$ kcal/mol and (b, bottom) $E_c = 13.6$ kcal/mol. The time scale is absolute, the ion flight time and electronic offsets having been taken into account. The distributions are normalized to the relative intensities at each angle. Solid lines: calculation with best-fit c.m. translational energy and angular distributions of Figure 3.

decrease of the cross section with increasing relative collision energy, and therefore, an $E_c^{-1/3}$ dependence has been used.

The c.m. product flux distribution is assumed to be separable into the product of a translational energy and an angular part, $I_{c.m.}(\theta,E'_T) = T(\theta)P(E'_T)$. The best fit calculations to the experimental angular and TOF distributions are shown as solid lines in Figures 1 and 2, respectively. Figure 3 shows the resultant c.m. angular distributions, $T(\theta)$, and translational energy distributions, $P(E'_T)$, for the two E_c. The final result of the data fitting analysis is a c.m. contour map of product flux as a function of angle and product recoil energy.[29] After a straightforward transformation to convert the flux distribution from an energy space to a velocity space, the c.m. contour maps $I_{c.m.}(\theta,u)$, where u is the c.m. product velocity, are represented in polar form in Figure 4. The transformation of the c.m. flux $I_{c.m.}(\theta,u)$ to laboratory number density $N(\Theta)$ is given[29] by $N(\Theta) = (v/u^2)I_{c.m.}(\theta,u)$. The effect of the Jacobian v/u^2 for the coordinate transformation results in a strong enhancement of the low-energy products. While the product flux actually peaks fairly well removed from the c.m. vector on the relative velocity axis (see Figure 4), the measured lab angular distributions do not show pronounced dips around $\Theta_{c.m.}$.

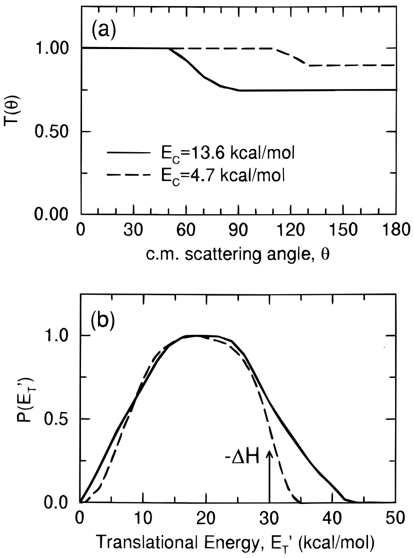

Figure 3. Best-fit center-of mass product angular (a) and translational energy (b) distributions. Solid lines: c.m. functions at $E_c = 13.6$ kcal/mol. Dashed lines: c.m. functions at $E_c = 4.7$ kcal/mol.

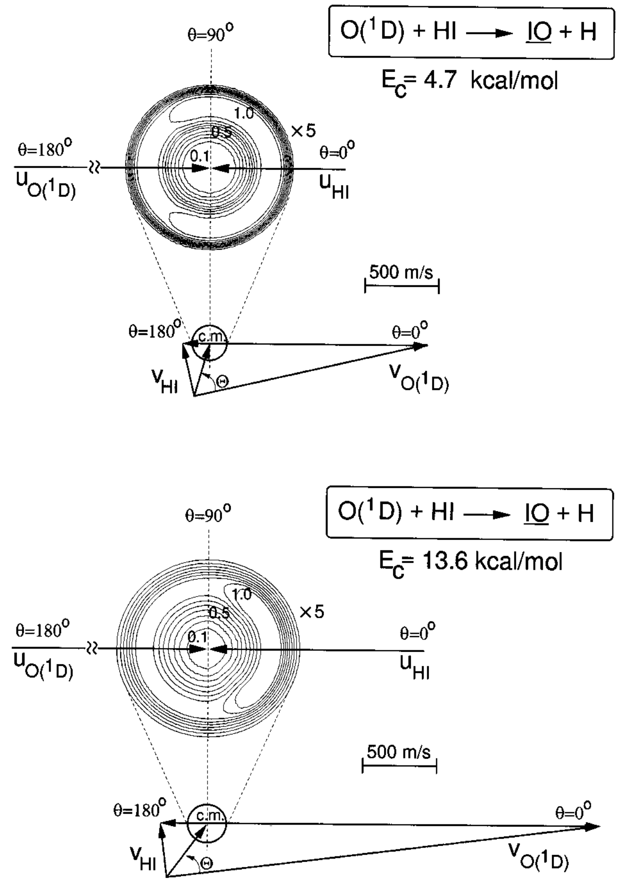

Figure 4. Center-of-mass polar flux (velocity−angle) contour maps of the IO product at $E_c = 4.7$ kcal/mol and $E_c = 13.6$ kcal/mol together with the most probable Newton diagrams (lab and c.m. velocities and angles are specified). The circles in the Newton diagrams delimit the maximum speed achievable by the IO product, assuming that all the available energy goes into product translation. The shift toward more forward scattering of the IO product with increasing E_c is clearly visible.

The two $P(E'_T)$ distributions are quite broad and peak at about the same value, which is ≈19 kcal/mol (see Figure 3b). The average product translational energy, defined as $\langle E'_T\rangle = \sum P(E'_T)E'_T/\sum P(E'_T)$, was determined to be 20 kcal/mol for the high-energy experiment and 19 kcal/mol for the low-energy experiment, that is almost the same despite the difference of about 9 kcal/mol in the collision energy. Therefore, the percentage of the total available energy, E_{tot}, released as product translational energy is somewhat different in the two cases. In this type of experiment, the total available energy is given by $E_{tot} = E_c - \Delta H°_r + E_{int}$, where $\Delta H°_r$ is the enthalpy of reaction and E_{int} is the internal energy of the reactants, namely, the internal energy of HI which can be neglected as we work with supersonic beams. The enthalpy of reaction is not accurately known, since the enthalpy of formation of the IO radical has not been accurately established yet. (See ref 31 for a recent review on the enthalpies of formation and other properties of iodine oxides.) The bond dissociation energy of IO, and hence the enthalpy of formation, have been calculated by many different techniques (the first estimate[32] goes back to 1948), but the various studies have not improved the reliability of the dissociation energy; the values reported in the literature range from $\Delta H°_{f,298} = 25.8$ kcal/mol to $\Delta H°_{f,298} = 41.1$ kcal/mol. Essentially, the derived values can be grouped in two types: a first group obtained from the treatment of spectroscopic data and a second group derived from dynamic and kinetic studies. The two groups are to some extent contradictory: while spectroscopic data have supported an enthalpy of formation of around 40 kcal/mol, molecular beam studies on the $O(^3P) + ICl$ reaction proposed $\Delta H°_{f,0} = 32.1 \pm 2.0$ kcal/mol[33] and $\Delta H°_{f,0} = 30.6 \pm 3.0$ kcal/mol.[34] Very recently, Ravishankara and co-workers[35] reported an upper limit of 28.8 kcal/mol and Bedjanian et al.[15h] an estimate of 26.7 ± 0.9 kcal/mol for $\Delta H°_{f,298}(IO)$. Quantum mechanical calculations performed by McGrath and Rowland[36] have recently provided a value of $\Delta H°_{f,0} = 31.0 \pm 1.0$ kcal/mol, while unpublished ab initio calculations by Johnson and co-workers[37] have given $\Delta H°_{f,0} = 28.7 \pm 1.2$ kcal/mol. Due to the large uncertainty over the enthalpy of formation of the IO radical, the $\Delta H°_r$ was treated as an adjustable parameter during the fitting procedure of the experimental data. In fact, it is possible, in principle, to determine the value of $\Delta H°_r$ from the falloff of the $P(E'_T)$, since the translational energy of the products cannot exceed the maximum total energy, due to the energy conservation relationship (see for instance ref 21b). Unfortunately, in our case crucial for the fitting of the experimental data were the rise and the peak position of the $P(E'_T)$ in both experiments, while the falloff, which is not sharp, can have slightly different slope without compromising the fitting main features. Another cause of uncertainty in the determination of the exact value of E_{tot} is due to the possibility of nonadiabatic coupling of the surfaces involved in the reaction, leading to the formation of IO also in the excited spin−orbit state $^2\Pi_{1/2}$. In a recent work on the related reaction $O(^1D) + HCl \rightarrow ClO + H$ at $E_c = 8.4$ kcal/mol, Matsumi and Shamsuddin[6e] have found a population ratio between $ClO(^2\Pi_{1/2})$ and $ClO(^2\Pi_{3/2})$ of 0.6, which is not statistical but witnesses extensive nonadiabatic coupling. The spin−orbit splitting of $IO(^2\Pi_{3/2,1/2})$ has been recently determined to be 2021 cm^{-1} ($\approx$6 kcal/mol);[38] due to the large atomic weight of iodine, spin conservation may be less rigid than for lighter systems, so that we expect nonadiabatic coupling even more extensive than in the case of $O(^1D) + HCl$. The value of $\Delta H°_r$ resulting from the best fit of our data is −30 kcal/mol for both experiments, leading to a $\Delta H°_{f,0}(IO) = 29$ kcal/mol, in agreement with the value derived by Grice and co-workers,[33] Lee and co-workers,[34] the very recent estimate of Ravishankara and co-workers,[35] and also the two recent theoretical determinations.[36,37] However, due to the low sensitivity of the fitting to the $P(E'_T)$ high-energy tail, we cannot rule out larger (up to 36 kcal/mol) and somewhat lower (up to 25 kcal/mol) values than 29 kcal/mol. Assuming $\Delta H°_r \approx -30$ kcal/mol, the fraction of energy released as translational energy of the products is 55% and 46% for the low and the high energy experiment, respectively.

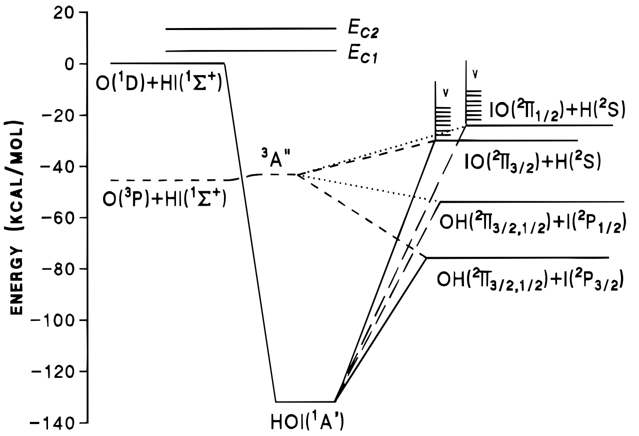

Figure 5. Energy level and correlation diagram for the $O(^3P,^1D) + HI$ system. E_{c1} and E_{c2} indicate the experimental relative collision energies. The fine structure states of the products are shown, with the exception of OH. The first vibrational states of IO are also shown. The energy barrier on the $^3A''$ surface (indicated with dashed line) has been made equal to the activation energy for the triplet reaction.

Discussion

In Figure 5 we show the energy level and correlation diagram which is relevant to the following discussion. The energy levels are known for the reactants, products, and the ground state of HOI.[39] Observations of gaseous HOI have been recently reported,[40] while formation of HOI was already observed in matrix experiments[41] and in aqueous phase;[42] the structure of HOI has been recently estimated by analyzing the spectra of vibrational hot HOI formed in the reaction of alkyl iodides with $O(^3P)$.[40a] In the related $O(^1D) + HX$ (X = Cl,Br) systems the first excited $^1A''$ PES and the ground X^1A' PES of HXO were thought to be energetically involved at the energies of the experiments, as suggested by SCF−CI calculations on the $O(^1D) + HCl$ system.[43] In the case of $O(^1D) + HI$, no information is available on the first electronically excited singlet surface of HOI; regarding the possible role of the isomer HIO, in theoretical studies Marshall and co-workers[44] have recently found the singlet HIO complex to be bound, although about 50 kcal/mol less stable than singlet HOI. In Figure 5 the barrier on the $^3A''$ surface has been indicated as equal to the activation energy of the ground state reaction. The c.m. angular and translational energy distributions for the IO + H channel shown in Figure 3 allow an evaluation of the dynamical influence of the PES and of kinematic constraints.

Angular Distributions. The best-fit c.m. angular distributions (Figure 3a) show intensity in the whole angular range, but they are not perfectly backward−forward symmetric, as one would expect if the reaction proceeded through a long-lived complex, i.e., a complex with a lifetime of several rotational periods.[45] The best-fit c.m. angular distribution at $E_c = 4.7$ kcal/mol is nearly isotropic with a slightly favored forward scattering with respect to the O atom direction ($T(180°)/T(0°) = 0.9$); indeed, a perfectly isotropic distribution would give more intensity in the backward direction of the calculated lab angular distribution than that resulting from the experiment. Actually, the calculated lab angular distribution shows somewhat lower intensities at angles close to the c.m.; an improvement can be achieved by using a c.m. $T(\theta)$ with a maximum barely visible at $\theta = 90°$ but with the same $T(180°)/T(0°)$ ratio. The best-fit c.m. angular distribution obtained at $E_c = 13.6$ kcal/mol shows a more pronounced preference for forward scattering, being $T(180°)/T(0°) = 0.75$. The asymmetry observed in both cases, and especially at the higher E_c, can be attributed to the fact that the reaction proceeds through the formation of a complex that decomposes within few rotational periods. In fact, according to the osculating complex model for chemical reaction,[46] a forward intensity enhancement is expected when the complex lifetime is a fraction of, or comparable to, its rotational period. An estimate of the lifetime for the complexes formed at the two collision energies can be obtained from the observed $T(\theta)$ asymmetry by means of $T(180°)/T(0°) = e^{-\tau_r/2\tau}$, where τ is the lifetime of the decomposing complex, τ_r is its rotational period, and $T(0°)$ and $T(180°)$ are the values assumed by the $T(\theta)$ function at the two poles.[46] The rotational period of the complex can be estimated from the relation $\tau_r = 2\pi I/L_{max}$, where I is the moment of inertia of the rotating complex and L_{max} is the maximum angular momentum. L_{max} is given by $\mu v_{rel} b_{max}$, where μ is the reduced mass of the reactants, v_{rel} is the initial relative velocity, and b_{max} is the maximum impact parameter. The value of b_{max} is not known for this reaction, since the opacity function has never been calculated. A rough estimate can be done by using the hard-sphere model,[30] $b_{max} = (\sigma_r/\pi)^{-1/2}$. The values of the reaction cross section σ_r at the two collision energies have been derived starting from the room-temperature rate constant, which, actually, has never been measured but can be inferred from the rate constants of the two analogous reactions $O(^1D) + HCl$ and $O(^1D) + HBr$. In fact, the measured rate coefficients for the two reactions are 1.50×10^{-10} and 1.48×10^{-10}cm^3 molecule^{-1} s^{-1}, respectively;[4a] these are quite typical values of room temperature k for $O(^1D)$ reactions with simple molecules, so that there is no reason to expect a significant variation for the rate coefficient of the next member along the $O(^1D) + HX$ series. The estimated values of σ_r are 12.2 Å^2 at $E_c = 4.7$ kcal/mol and 8.6 Å^2 at $E_c = 13.6$ kcal/mol, and the resulting L_{max} are 7.74×10^{-26} and 1.10×10^{-25} g cm^2 s^{-1}. Assuming that the complex formed during the reaction following $O(^1D)$ insertion into the H−I bond is HOI and using the moments of inertia recently determined by Leone and coworkers,[40a] the resulting lifetimes are ≈4 ps at $E_c = 4.7$ kcal/mol and ≈1 ps at $E_c = 13.6$ kcal/mol. The approximations required to extract complex lifetimes from the experimental data are numerous, but at least the ratio τ/τ_r, which is 4.7 and 1.7 in the two cases, should be regarded as realistic.

In the case of the related $O(^1D) + HCl$ and HBr reactions the c.m. angular distributions were found to be somewhat backward biased, and they were assumed to arise from the superposition of a backward−forward symmetric component and a backward scattered component.[5,7] In the case of $O(^1D) + HBr$ it was actually necessary to separate these two contributions to fit the data: the backward−forward component was related to the formation of a long-lived complex via an insertion mechanism, forming the strongly bound $HOBr(X^1A')$ intermediate; the backward scattered component was attributed to reactive encounters taking place by nearly collinear collisions of the oxygen from the Br side of HBr at small impact parameters.[7] The direct abstraction of the halogen atom with rebound dynamics witnessed the role played by H−X−O configurations. This backward contribution amounts to about 15% in the case of HBr[7] and is presumably similar in the case of HCl, since the shape of the $T(\theta)$ function is also similar in the two systems at comparable E_c. Interestingly, no backward component is instead observed in the reaction with HI, suggesting that the direct abstraction of the iodine atom plays a negligible role. In particular, the formation of an osculating complex in the case of HI indicates a smaller τ/τ_r for HOI with respect to HOCl and HOBr at comparable energies, which may not be surprising considering that both competitive dissociation channels of the complex are significantly more exoergic for $O(^1D) + HI$ than for $O(^1D) + HCl$ and $O(^1D) + HBr$. The reason for the lack of backward scattering component in $O(^1D) + HI \rightarrow IO + H$ may lie in the stronger long-range attractive interaction between the oxygen atom and the HI molecule, with the $O(^1D)$ atom driven into the deep H−O−I well whatever its attack orientation. Another possibility is that when $O(^1D)$ approach HI from the halogen side the formed HIO is also a long-lived complex, which can dissociate directly to IO + H or isomerize to HOI before dissociating.

The relative peaking of the $T(\theta)$ function at the poles ($\theta = 0°$ and 180°) with respect to $\theta = 90°$ provides information about the disposal of the total angular momentum into product rotation.[45] In the present case a very weak polarization is found (see Figure 3a), weaker than in the case of $O(^1D) + HCl$[5] and comparable to the case of $O(^1D) + HBr$.[7] For this specific mass combination, angular momentum partitioning arguments predict very high product rotational excitation. In fact, as a consequence of the much smaller reduced mass of the products with respect to that of the reagents, the final orbital angular momentum $\mathbf{L}'$ is much smaller than the initial one $\mathbf{L}$, and the final rotational angular momentum $\mathbf{j}'$ is about equal to $\mathbf{L}$. (The initial $\mathbf{j}$ is very small with respect to $\mathbf{L}$, in view of the fact that reagent molecules are formed in a supersonic expansion where considerable rotational cooling occurs, and can be neglected.) In the absence of a preferred dissociation geometry, high product rotational excitation leads ultimately to an isotropic c.m. angular distribution. In fact, one would observe a $T(\theta)$ sharply polarized at $\theta = 0°$ and $\theta = 180°$ only if $\mathbf{L}'$ and $\mathbf{L}$ are parallel or antiparallel. This situation occurs when the product molecules are not rotationally excited or when M′ (which is the projection of the total angular momentum $\mathbf{J} = \mathbf{L} + \mathbf{j} = \mathbf{L}' + \mathbf{j}'$ along the final recoil velocity vector $\mathbf{v}'$) is null.[45] In all the other cases, i.e., when part of the total angular momentum is removed as $\mathbf{j}'$ and M′ is not null, $\mathbf{L}$ and $\mathbf{L}'$ are weakly correlated and the recoil velocity vector $\mathbf{v}'$ *emerges out* of the collision plane, and therefore the condition for sharp polarization at the poles is removed, while the backward−forward symmetry is maintained. From the condition $\mathbf{L} \cong \mathbf{J} = \mathbf{L}' + \mathbf{j}'$ in the O + HX series, one expects the largest $\mathbf{j}'$, and then the highest rotational excitation, for the case of IO since the difference between $\mu'(IO + H)$ and $\mu(O + HI)$ is the largest; hence, $\mathbf{L} >> \mathbf{L}'$ and most of the total angular momentum is taken away from the rotation of the molecules, i.e., $\mathbf{j}' \cong \mathbf{L}$.

Product Energy Distributions. A common feature of the XO (X = Cl, Br, I) + H reaction channel is the large fraction (about 50%) of the total available energy released into product translation. This fraction is somewhat larger than that predicted by the RRHO microcanonical prior distribution of Levine and Bernstein[30] for these systems and may be taken as an indication of the presence of a small potential barrier in the exit valley, as suggested by classical trajectory studies[47] on model surfaces for the H + HL → HH + L (H = heavy, L = light) mass combination. Interestingly, recent ab initio and model calculations of the PES found a barrier for dissociation of HClO[9a,b] and also of HBrO;[48] it is reasonable to expect an exit barrier for dissociation of HIO as well. This suggests that HIO complexes actually play a role in the $O(^1D) + HI \rightarrow IO + H$ reaction.

It is interesting to note that both $P(E'_T)$ distributions (Figure 3b) peak at a value of about 19 kcal/mol, which is significantly lower than the exoergicity of the reaction ($\Delta H_r = -30$ kcal/mol), while for the reactions with HCl and HBr the corresponding $P(E'_T)$ peaked beyond the reaction exoergicity. However, while for $O(^1D) + HBr$ the $\langle E'_T\rangle$ fraction did not vary with E_c, for $O(^1D) + HI$ it decreases considerably with increasing E_c (from 55% to 46%), which indicates that the extra initial translational energy is more efficiently channeled into internal energy. Since a very large fraction of the available energy is released as product translation and high rotational excitation also occurs (assuming $\mathbf{j}' = \mathbf{L}$, it can be estimated an average product rotational energy $\langle E'_R\rangle$ of 5.3 and 10.6 kcal/mol at low and high E_c, respectively), little energy remains for electronic and vibrational excitation of the IO product. Since the spin–orbit splitting of IO is 6 kcal/mol and the vibrational spacing about 2 kcal/mol, IO should be mainly formed in the lowest few vibrational levels of both possible $^2\Pi_{1/2}$ and $^2\Pi_{3/2}$ states. Unfortunately, in the present experiment the relative population of the fine structure levels of IO could not be disentangled during the data analysis.

Branching Ratio σ(IO + H)/σ(OH + I). A lower limit for the ratio between the cross section, σ, for formation of XO and OH for the analogous $O(^1D) + HCl$[5a] and $O(^1D) + HBr$[7] reactions was estimated to be $\sigma(ClO + H)/\sigma(OH + Cl) = 0.34 \pm 0.10$ and $\sigma(BrO + H)/\sigma(OH + Br) = 0.16 \pm 0.07$. For X = I no estimate was attempted, because the sensitivity to the OH formation channel decreases as the halogen atom mass increases, due to the very unfavorable kinematics. Kinematically, it should be more convenient to detect the I atom than the OH counterpart, but unfortunately, I^+ produced from dissociative ionization, under electron impact in the detector, of elastically scattered HI represents a severe complication. However, on the basis of the relative signal intensities observed ($S(IO) \approx 2.5S(BrO) \approx 7S(ClO)$ under approximately the same experimental conditions), it is inferred that the IO formation channel should be as important as the BrO and ClO formation channels and, therefore, a significant fraction of the corresponding overall $O(^1D) + HI$ reaction. The findings for X = Cl, Br were in agreement with bulk estimates.[4]

Conclusion

The dynamics of the $O(^1D) + HI$ reaction relative to the H-displacement channel is found to resemble those of the analogous $O(^1D) + HCl$ and $O(^1D) + HBr$ reactions, but with the noteworthy difference that no evidence for a direct rebound mechanism arising from collinear attack of the oxygen atom on the halogen side of the hydride is observed in this case. IO formation is found to occur via an osculating complex, whose lifetime decreases with increasing collision energy. Complex formation arises likely from an insertion mechanism involving the ground state PES X^1A' of HOI and/or from an addition mechanism leading to HIO, which may subsequently isomerize to HOI or directly dissociate to IO + H. Interestingly, the dynamics of the reaction $O(^1D) + HI \rightarrow IO + H$ are very similar to those of $O(^1D) + H_2S \rightarrow HSO + H$, where the absence of a backward scattered component was also noted and the complex lifetime was decreasing with increasing E_c.

No information is available on the OH forming channel. In the two other reactions of the series, spectroscopic studies[6,7] found OH to be formed highly vibrationally and rotationally excited. The explanation proposed was that the reactions proceed through the insertion of $O(^1D)$ into the H–X bond on the $^1A'$ surface with formation of an internally hot HOX complex, which fragments within a few bending vibrations into OH + X, before the randomization of energy is complete. The OH forming channel in all the $O(^1D)$ reactions studied to date by using infrared chemiluminescence or laser-induced fluorescence has been found to have a nonstatistical product internal energy distribution, indicating that complete energy randomization does not occur within the complex lifetime; however, this does not necessarily indicate that the complex lifetime is short in comparison to its average rotational period.[6f,19d]

Our results on the H-displacement channel examined in this and in other related systems indicate that the reactions proceed mainly through the formation of a collision complex living a few rotational periods. When X changes along the series Cl, Br, and I, the two possible XO and OH forming channels become more exoergic, and the complex lifetime decreases with respect to its rotational period. The present experimental results complement the dynamical information obtained on the other members of the $O(^1D) + HX$ series and should facilitate attempts to model the dynamics of these reactions using realistic PESs. An accurate description of the fate of the presumably formed HOX/HXO complexes will be possibly given by quasiclassical trajectory and quantum mechanical dynamics calculations when they will become available. Theoretical work along these lines has recently appeared in the literature for the $O(^1D) + HCl$ reaction,[9a,b] is in progress for $O(^1D) + HBr$,[48] and is being planned for $O(^1D) + HI$.[49]

Acknowledgment. We acknowledge useful discussions with Prof. J. M. Farrar, Prof. J. J. Sloan, and Prof. A. Laganà. We thank Prof. P. Marshall for communicating to us his results prior to publication. Also, we thank an anonymous referee for useful comments and suggestions. This work has been supported by the Italian "Consiglio Nazionale delle Ricerche—Progetto Finalizzato Chimica Fine" and "Ministero Università e Ricerca Scientifica". Grants from NATO (CRG 920549) and AFOSR (F617-08-94-C-0013) through EOARD (SPC-94-4042) made possible several aspects of the research reported here.

References and Notes

(1) (a) Ravishankara, A. R.; Smith, G.; Watson, R. T.; Davis, D. D. *J. Phys. Chem.* **1977**, *81*, 2220. (b) Mahmud, K.; Kim, J. S.; Fontijn, A. *J. Phys. Chem.* **1990**, *94*, 2994.

(2) (a) Brown, R. D. H.; Smith, I. W. M. *Int. J. Chem. Kinet.* **1975**, *7*, 301; **1978**, *10*, 1. (b) Nava, D. F.; Bosco, S. R.; Stief, L. J. *J. Chem. Phys.* **1983**, *78*, 2443.

(3) Singleton, D. L.; Cvetanovic, R. J. *Can. J. Chem.* **1978**, *56*, 2934.

(4) (a) Wine, P. H.; Wells, J. R.; Ravishankara, A. R. *J. Chem. Phys.* **1986**, *84*, 1349. (b) Wine, P. H. Private communication.

(5) (a) Balucani, N.; Beneventi, L.; Casavecchia, P.; Volpi, G. G. *Chem. Phys. Lett.* **1991**, *180*, 34. (b) Balucani, N.; Beneventi, L.; Casavecchia, P.; Stranges, D.; Volpi, G. G. In *Ecological Physical Chemistry*; Rossi, C.; Tiezzi, E., Eds.; Elsevier: Amsterdam, 1991; p 539.

(6) (a) Luntz, A. C. *J. Chem. Phys.* **1980**, *73*, 5393. (b) Kruus, E. J.; Niefer, B. I.; Sloan, J. J. *J. Chem. Phys.* **1988**, *88*, 985. (c) Park, C. R.; Wiesenfeld, J. R. *Chem. Phys. Lett.* **1989**, *163*, 230. (d) Matsumi, Y.; Tarokura, K.; Kawasaki, M.; Tsuji, K.; Obi, K. *J. Chem. Phys.* **1993**, *98*, 8330. (e) Matsumi, Y.; Shamsuddin, S. M. *J. Chem. Phys.* **1995**, *103*, 4490. (f) Alexander, A. J.; Brouard, M.; Rayner, S. P.; Simons, J. P. *Chem. Phys.* **1996**, *207*, 215.

(7) Balucani, N.; Beneventi, L.; Casavecchia, P.; Volpi, G. G.; Kruus, E. J.; Sloan, J. J. *Can. J. Chem.* **1994**, *72*, 888.

(8) (a) McKendrick, K. G.; Rakestraw, D. J.; Zhang, R; Zare, R. N. *J. Phys. Chem.* **1988**, *92*, 5530. (b) Zhang, R.; van der Zande, W. J.; Bronikowski, M. J.; Zare, R. N. *J. Chem. Phys.* **1991**, *94*, 2704.

(9) (a) Laganà, A.; Ochoa de Aspuru, G.; Garcia, E. *J. Phys. Chem.* **1995**, *99*, 17139. (b) Hernandez, M. L.; Redondo, C.; Laganà, A.; Ochoa de Aspuru, G.; Rosi, M.; Sgamellotti, A. *J. Chem. Phys.* **1996**, *105*, 2710. (c) Schinke, R. *J. Chem. Phys.* **1984**, *80*, 5510. (d) Koizumi, H.; Schatz, G. C.; Gordon, M. S. *J. Chem. Phys.* **1991**, *95*, 6421.

(10) Agrawalla, B. S.; Manocha, A. S.; Setser, D. W. *J. Phys. Chem.* **1981**, *85*, 2873.

(11) Persky, A.; Broida, M. *Chem. Phys.* **1987**, *114*, 85.

(12) Alagia, M.; Balucani, N.; Casavecchia, P.; Laganà, A.; Ochoa de Aspuru, G.; van Kleef, E. H.; Volpi, G. G.; Lendvay, G. *Chem. Phys. Lett.* **1996**, *258*, 323.

(13) Atkinson, R.; Baulch, D. L.; Cox, R. A.; Hampson, R. F., Jr.; Kerr, J. A.; Troe, J. *J. Phys. Chem. Ref. Data* **1992**, *21*, 1125.

(14) Chameides, W. L.; Davis, D. D. *J. Geophys. Res.* **1980**, *85*, 7383.

(15) (a) Jenkin, M. E.; Cox, R. A. *J. Phys. Chem.* **1985**, *89*, 192. (b) Sander, S. P. *J. Phys. Chem.* **1986**, *90*, 2194. (c) Stickel, R. E.; Hynes, A. J.; Bradshaw, J. D.; Chameides, W. L.; Davis, D. D. *J. Phys. Chem.* **1988**, *92*, 1862. (d) Daykin, E. P.; Wine, P. H. *J. Phys. Chem.* **1990**, *94*, 4528. (e) Mac Leod, H.; Balestra, C.; Jourdain, J. L.; Laverdet, G.; Le Bras, G. *Int. J. Chem. Kinet*. **1990**, *22*, 1167. (f) Maguin, F.; Laverdet, G.; Le Bras, G.; Poulet, G. *J. Phys. Chem.* **1992**, *96*, 1775. (g) Turnipseed, A. A.; Gilles, M. K.; Burkholder, J. B.; Ravishankara, A. R. *Chem. Phys. Lett.* **1995**, *242*, 427. (h) Bedjanian, Y.; Le Bras, G.; Poulet, G. *J. Phys. Chem.* **1996**, *100*, 15130. (i) Harwood, M. H.; Burkholder, J. B.; Hunter, M.; Fox, R. W.; Ravishankara, A. R. *J. Phys. Chem. A* **1997**, *101*, 853.

(16) (a) Solomon, S.; Garcia, R. R.; Ravishankara, A. R. *J. Geophys. Res.* **1994**, *99* (D10), 20491. See also: (b) Solomon, S.; Burkholder, J. B.; Ravishankara, A. R.; Garcia, R. R. *J. Geophys. Res.* **1994**, *99* (D10), 20929.

(17) Sloan, J. J. *J. Phys. Chem.* **1988**, *92*, 18.

(18) van Zee, R. D.; Stephenson, J. C. *J. Chem. Phys*. **1995**, *102*, 6946.

(19) (a) Luntz, A. C. *J. Chem. Phys*. **1980**, *73*, 1143. (b) Aker, P. M.; O'Brien, J. J. A.; Sloan, J. J. *J. Chem. Phys*. **1986**, *84*, 745. (c) Park, C. R.; Wiesenfeld, J. R. *J. Chem. Phys*. **1991**, *95*, 8166. (d) Brouard, M.; Duxon, S.; Enriquez, P. A.; Simons, J. P. *J. Chem. Soc.*, *Faraday Trans.* **1993**, *89*, 1435.

(20) Alagia, M.; Balucani, N.; Cartechini, L.; Casavecchia, P.; G.; van Kleef, E. H.; Volpi, G. G.; Kruus, P. J.; Sloan, J. J. Manuscript in preparation.

(21) (a) Balucani, N.; Beneventi, L.; Casavecchia, P.; Stranges, D.; Volpi, G. G. *J. Chem. Phys.* **1991**, *94*, 8611. (b) Balucani, N.; Casavecchia, P.; Stranges, D.; Volpi, G. G. *Chem. Phys. Lett.* **1993**, *211*, 469. (c) Balucani, N.; Casavecchia, P.; Stranges, D.; Volpi, G. G. Manuscript in preparation.

(22) Alagia, M.; Balucani, N.; Cartechini, L.; Casavecchia, P.; van Beek, M. C.; Volpi, G. G., Manuscript in preparation.

(23) Lee, Y. T.; McDonald, J. D.; LeBreton, P. R.; Herschbach, D. R. *Rev. Sci. Instrum.* **1969**, *40*, 1402.

(24) Sibener, S. J.; Buss, R. J.; Ng, C. Y.; Lee, Y. T. *Rev. Sci. Instrum.* **1980**, *51*, 167.

(25) (a) Beneventi, L.; Casavecchia, P.; Volpi, G. G. *J. Chem. Phys.* **1986**, *85*, 7011. (b) Beneventi, L.; Casavecchia, P.; Volpi, G. G., Bieler, C. R.; Janda, K. C. *J. Chem. Phys.* **1993**, *98*, 178 and references therein.

(26) (a) Casavecchia, P.; Balucani, N.; Volpi, G. G. In *Research in Chemical Kinetics*; Compton, R. G., Hancock, G., Eds.; Elsevier: Amsterdam, 1993; Vol. 1, p 1. (b) Casavecchia, P.; Balucani, N.; Volpi, G. G. In *Advanced Series in Physical Chemistry*; Wagner, A., Liu, K., Eds.; Worlds Scientific: Singapore, 1995; Vol. 6, p 365. (c) Alagia, M.; Balucani, N.; Casavecchia, P.; Stranges, D.; Volpi, G. G. *J. Chem. Soc.*, *Faraday Trans.* **1995**, *91*, 575.

(27) Sköld, K. *Nucl. Instrum. Methods* **1968**, *63*, 114.

(28) Buss, R. J. Ph.D. Thesis, University of California, Berkeley, 1979.

(29) Lee, Y. T. In *Atomic and Molecular Beam Methods*: Scoles, G., Ed.; Oxford Univesity Press: New York, 1987; Vol. 1.

(30) Levine, R. D.; Bernstein, R. B. *Molecular Reaction Dynamics*; Oxford Univesity Press: Oxford, 1974.

(31) Chase, M. W. *J. Phys. Chem. Ref. Data*, **1996**, *25*, 1297 and references therein.

(32) Coleman, E. H.; Gaydon, A. G.; Vaidya, W. M. *Nature* **1948**, *162*, 108.

(33) Radlein, D. St. A. G.; Whitehead, J. C.; Grice, R. *Nature* **1975**, *253*, 5486.

(34) Buss, R. J.; Sibener, S. J.; Lee, Y. T. *J. Phys. Chem.* **1983**, *87*, 4840.

(35) Gilles, M. K.; Turnipseed, A. A.; Rudich, Y.; Talukdar, R. K.; Villalta, P.; Huey, L. G.; Burkholder, L. B.; Ravishankara, A. R. *J. Phys. Chem.* **1996**, *100*, 14005.

(36) McGrath, M. P.; Rowland, F. S. *J. Phys. Chem.* **1996**, *100*, 4815.

(37) Hassanzadeh, P. H.; Irakura, K. K.; Johnson, R. D. III Unpublished data; see ref 31.

(38) (a) Bekoy, J. P.; Leo Meerts, W.; Dymanus, A. *J. Mol. Spectrosc.* **1983**, *102*, 320. (b) Gilles, M. K.; Polak, M. L.; Lineberger, W. C. *J. Chem. Phys.* **1991**, *95*, 4723; **1992**, *96*, 8012.

(39) About the enthalpy of formation of HOI we refer to the value reported in; Loewenstein, L. M.; Anderson, J. G. *J. Phys. Chem.* **1987**, *91*, 2993.

(40) (a) Klaassen, J. J.; Lindner, J.; Leone, S. R. *J. Chem. Phys.* **1996**, *104*, 7403. (b) Barnes, I.; Becker, K. H.; Starke, J. *Chem. Phys. Lett.* **1992**, *196*, 578. (c) Jenkin, M. E.; Clemitshaw, K. C.; Cox, R. A. *J. Chem. Soc.*, *Faraday Trans. 2* **1984**, *80*, 1633.

(41) Walker, N.; Tevault, D. E.; Smardzewski, R. R. *J. Chem. Phys.* **1978**, *69*, 564.

(42) Pasquette, J.; Ford, B. L. *Can. J. Chem.* **1985**, *63*, 2444.

(43) Bruna, P. J.; Horsch, G.; Peyerimhoff, S. D.; Buenker, R. J. *Can. J. Chem.* **1979**, *57*, 1839.

(44) Marshall, P. Private communication.

(45) Miller, W. B.; Safron, S. A.; Herschbach, D. R. *Discuss. Faraday Soc.* **1967**, *44*, 108.

(46) Fisk, G. A.; McDonald, J. D., Herschbach, D. R. *Discuss. Faraday Soc.* **1967**, *44*, 228.

(47) Polanyi, J. C.; Schreiber, J. L. In *Physical Chemistry: An Advanced Treatise*, Jost, W., Ed.; Academic Press: New York, 1974; Vol. 6A, p 383.

(48) Ochoa de Aspuru, G. Ph.D. Thesis, Universidad del Pais Vasco, 1996. Laganà, A.; Ochoa de Aspuru, G.; Garcia, E. Manuscript in preparation.

(49) Laganà, A. Private communication.